Hydration of denatured and molten globule proteins

Vladimir P. Denisov[1], Bengt-Harald Jonsson[2] and Bertil Halle[1]

The hydration of nonnative states is central to protein folding and stability but has been probed mainly by indirect methods. Here we use water ^{17}O relaxation dispersion to monitor directly the internal and external hydration of α-lactalbumin, lysozyme, ribonuclease A, apomyoglobin and carbonic anhydrase in native and nonnative states. The results show that nonnative proteins are more structured and less solvent exposed than commonly believed. Molten globule proteins preserve most of the native internal hydration sites and have native-like surface hydration. Proteins denatured by guanidinium chloride are not fully solvent exposed but contain strongly perturbed occluded water. These findings shed new light on hydrophobic stabilization of proteins.

The current view of protein folding and stability is largely based on a generic structural classification into native (N), compact denatured or molten globule (MG), and unfolded or denatured (D) conformational states[1–10]. Whereas the N state has been characterized at high resolution, many aspects of the D and MG states are still poorly understood. Considering the widely acknowledged importance of protein–solvent interactions for stability and folding, remarkably little is known about nonnative protein hydration. Structural studies of the D and MG states have naturally focused on the properties of the polypeptide chain; its degree of compactness, secondary structure, tertiary fold, and side-chain packing. Inferences about hydration have usually been indirect (where the peptide chain is not, there is solvent) or have relied on uncertain premises. Small-angle X-ray scattering (SAXS), dynamic light scattering (DLS), optical rotation and viscosity data have often been taken to indicate that the D state induced by strong denaturants (and disulfide reduction) approaches a random coil[1], implying that the polypeptide chain is exposed to bulk solvent. This view of the D state is implicit in all solution transfer models of protein stability[11,12]. Evidence is mounting, however, for residual nonrandom structure in the D state of many proteins[3,6,9]. For the N → MG transition, the typical 30% volume expansion derived from SAXS and DLS data[13–16] and the extensive exposure of hydrophobic residues suggested by the finding that the heat capacity of the MG state is midway between that of the N and D states[7] have been taken to imply that hundreds of water molecules penetrate the MG protein (except for a relatively small hydrophobic core)[5,7,8,17–19]. Accordingly, theoretical models of the MG state invariably invoke a substantial internal hydration[20–22].

Protein hydration, even for the N state, has long been shrouded in controversy[23]. In recent years, however, high-resolution ^{1}H nuclear Overhauser effect (NOE) spectroscopy[24] and ^{17}O magnetic relaxation dispersion (MRD)[25] have provided unambiguous structural and dynamic information about the internal (buried) and external (surface) hydration of globular proteins in solution. These two NMR techniques are largely complementary; while the MRD method lacks the intrinsic spatial resolution of the NOE method, it provides more direct information about the extent (number of water molecules), order (orientational order parameter) and dynamics (rotational correlation time and residence time) of hydration water. Moreover, slow conformational exchange and side-chain disorder, which severely impair the resolution in ^{1}H spectra of nonnative proteins, do not pose any problems in MRD work.

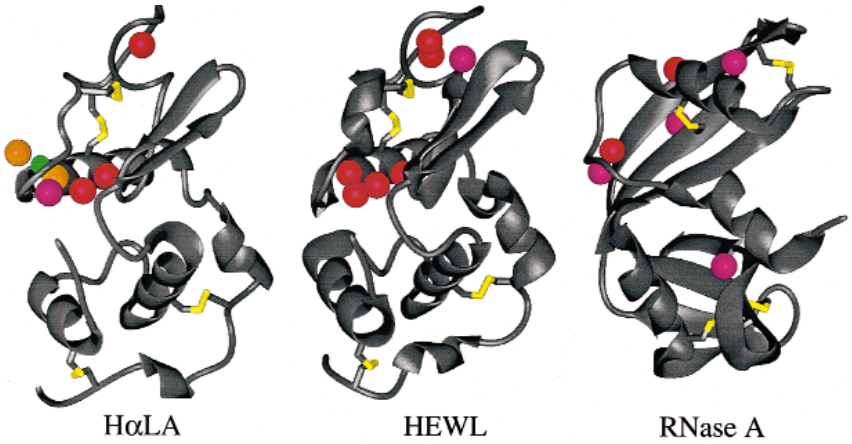

Fig. 1 Crystal structures of human α-lactalbumin (PDB file 1HML), lysozyme (2LZT) and ribonuclease A (7RSA) showing potentially long-lived internal water molecules, disulfide bonds (yellow), and the Ca^{2+} ion (green) in α-lactalbumin. All displayed water molecules have thermal B-factors <20 Å^2 and are extensively hydrogen bonded[27]; they are colored red (buried, solvent-accessible area, A_S = 0), magenta (partly buried, A_S <10 Å^2), or orange (metal coordinated). For α-lactalbumin, only water molecules conserved in the human and baboon structures are shown (the structure of the bovine protein has not been reported).

[1]Condensed Matter Magnetic Resonance Group, Department of Chemistry, Lund University, S-22100 Lund, Sweden. [2]Department of Biochemistry, Umeå University, S-90187 Umeå, Sweden.

Correspondence should be addressed to B.H. *email: bertil.halle@fkem2.lth.se*

Table 1 Hydration parameters derived from ^{17}O MRD data from solutions of native, denatured and molten globule proteins

Protein	State[1]	C_p[2] (mM)	pH*	[GdmCl] (M)	$N_\alpha\rho_\alpha$ (10^3)	$N_\beta S_\beta^2$	τ_β (ns)
BαLA	N	1.9	8.4	–	1.83 ± 0.16	3.2 ± 0.2	6.9 ± 0.4
	D	1.9	7.0	4.4	3.60[3]	0.37 ± 0.08	6.8 ± 1.9
	DR	1.9	7.0	4.4	3.60 ± 0.04	–	–
	MG	1.9	2.0	–	2.0 ± 0.2	1.6 ± 0.2	7.4 ± 0.8
HEWL	N	7.0	4.4	–	1.8 ± 0.2	2.7 ± 0.4	5.3 ± 0.6
	D	3.9	5.0	7	2.30[3]	0.45 ± 0.10	4.2 ± 1.2
	DR	3.9	5.0	7	2.30 ± 0.05	–	–
RNase A	N	3.8	4.0	–	2.1 ± 0.1	2.3 ± 0.3	3.6 ± 0.3
	D	3.8	4.0	4	2.52 ± 0.03	0.21 ± 0.06	5.6 ± 1.3
	DR	3.8	4.0	4	3.59 ± 0.02	–	–
apoMb	N	2.0	5.9	–	2.8 ± 0.2	1.26 ± 0.17	8.8 ± 1.2
	MG	2.0	4.3	–	2.5 ± 0.1	0.81 ± 0.11	8.9 ± 1.1
	D	2.0	2.2	–	1.80 ± 0.06	0.33 ± 0.05	10.6 ± 1.7
HCAII	N	2.5	9.0	–	7.0 ± 0.4[4]	8.1 ± 1.2[4]	11 ± 6[4]
	D	2.2	8.7	4	10.5 ± 0.6	–	–
	MG	0.75	3.0	–	6.9 ± 0.3[4]	9.1 ± 0.4[4]	26 ± 3[4]

[1]N, native; D, denatured; DR, denatured and reduced; MG, molten globule.
[2]Protein concentration (before addition of dry GdmCl).
[3]Parameter value frozen in the fit.
[4]Average parameters obtained from bilorentzian fit to longitudinal and transverse MRD data.

A recent study of thermally denatured bovine ribonuclease A (RNase A) demonstrated the potential of the MRD method for characterizing the hydration (and side-chain flexibility) of nonnative proteins[26]. Here we report the results of a water ^{17}O MRD study of eight isothermally prepared nonnative protein states: the acid-induced MG states of bovine α-lactalbumin (BαLA), horse apomyoglobin (apoMb) and human carbonic anhydrase II (HCAII), the guanidinium chloride (GdmCl)-induced denatured (D) and denatured-reduced (DR) states of hen lysozyme (HEWL), BαLA, RNase A and HCAII, and the acid-denatured state of apoMb. For reference, we also studied the N state of these five proteins as well as amino acid mixtures. To our knowledge, this is the first direct study of the state of water interacting with nonnative proteins in molten globule and extensively solvent-denatured states.

Our results indicate that nonnative proteins are more structured and less hydrated than commonly believed. The three investigated MG proteins all contain long-lived (>10 ns) water molecules in numbers comparable to the N state, indicating native-like and persistent tertiary structure at these internal locations. Furthermore, we find no support for the view that the N → MG transition is accompanied by a massive influx of water. For the three investigated proteins, the surface hydration of the MG state closely resembles that of the N state.

Surprisingly, BαLA, HEWL and RNase A were all found to contain long-lived (internal) water in the fully GdmCl-denatured state, indicating persistent residual structure. For each of these proteins, disruption of the four disulfide bonds eliminated the long-lived hydration sites. In contrast, the GdmCl-denatured state of HCAII contains no long-lived water, consistent with the absence of disulfide bonds in this protein. According to the MRD results, the external hydration of acid-denatured apoMb resembles that of a fully solvent-exposed polypeptide chain, whereas the GdmCl-denatured and disulfide-reduced proteins seem to adopt a more compact structure where the occluded water is more dynamically perturbed. The present MRD results on the hydration of nonnative proteins are at variance with the usual interpretation of volumetric and calorimetric data and have important implications for the understanding of protein stability and folding.

Internal and external hydration of native proteins

Measurements of the water ^{17}O longitudinal relaxation rate, R_1, over a wide frequency range can discriminate between internal hydration by water molecules trapped in cavities or deep surface pockets and external hydration by water molecules in contact with the protein surface[25]. This discrimination is based on the water residence time, τ_W, that is, the mean time that a particular water molecule occupies a given site. Only water molecules with τ_W longer than ~1 ns contribute significantly to the frequency dependence of R_1 (the relaxation dispersion). The dispersion frequency yields the correlation time $\tau_\beta = (1/\tau_R + 1/\tau_W)^{-1}$, where τ_R is the rotational correlation time of the protein (5–10 ns here), while the magnitude of the dispersion step provides the product, $N_\beta S_\beta^2$, of the number, N_β, and mean-square orientational order parameter, S_β^2, of long-lived water molecules (see Methods). Previous MRD studies of native proteins have established that internal water molecules (buried or otherwise trapped) are sufficiently long-lived to contribute to the dispersion[27,28]. The potentially long-lived water molecules can usually be identified from high-resolution crystal structures, as illustrated in Fig. 1 for three of the proteins studied here.

At frequencies above the dispersion region, the relaxation rate remains well above the bulk solvent value. This high-frequency relaxation enhancement is due to a large number, N_α (~500 for a 15 kDa protein) of short-lived (τ_W <1 ns) water molecules in contact with the protein surface. The MRD data provide a global measure of this external hydration in the form of the product $N_\alpha\rho_\alpha$, involving the relative dynamic retardation $\rho_\alpha = (\tau_\alpha / \tau_{bulk}-1)$, with τ_α the rotational correlation time averaged over all surface sites and τ_{bulk} the rotational correlation time in the bulk solvent (~3 ps in D_2O at 27 °C).

As a reference point, we consider first the hydration of native proteins. Provided here are the ^{17}O MRD profiles of the native forms of BαLA, HEWL and RNase A (Fig. 2). The quantities $N_\alpha\rho_\alpha$, $N_\beta S_\beta^2$ and τ_β derived from these profiles (see Methods) are listed in Table 1. These three proteins have similar mass (13.7–14.2 kDa), volume (16.2–16.4 nm^3) and solvent-accessible surface area (65.1–71.5 nm^2), and all have four disulfide bonds. They also have similar amounts of internal hydration, with six to seven potentially long-lived water molecules (Fig. 1). The magnitude of the dispersion step, proportional to the product of $N_\beta S_\beta^2$ and τ_β (see equation 1), is smallest for RNase A since all of its six potentially long-lived water molecules reside in surface pockets and, consequently, have relatively short residence times, τ_W = 8 ns at 27 °C[26], accounting for the short τ_β in Table 1. BαLA and HEWL have closely similar $N_\beta S_\beta^2$ values, despite the presence of two calcium-bound water molecules (presumably long-lived[29]) in BαLA. As expected from their structural homology, BαLA and HEWL have identical external hydration ($N_\alpha\rho_\alpha$), slightly smaller than for RNase A. Estimating N_α by dividing the solvent-accessible surface area by 15 $Å^2$, we obtain a

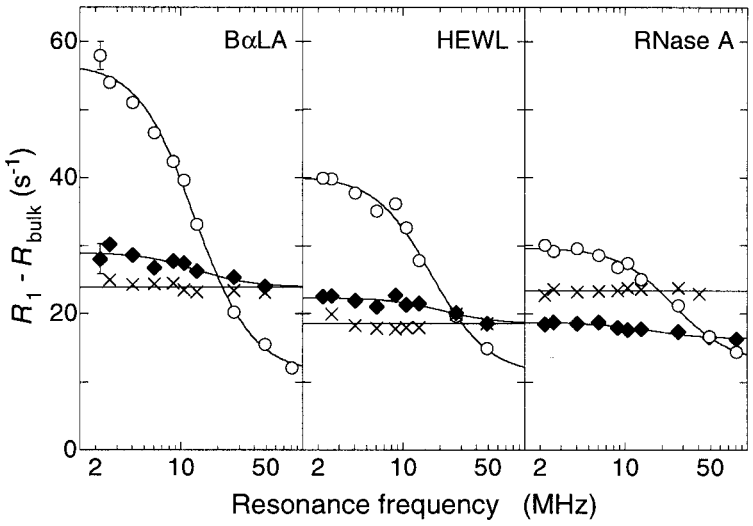

Fig. 2 Frequency dependence of water ^{17}O excess longitudinal relaxation rate from solutions of α-lactalbumin, lysozyme and ribonuclease A in the native (○), GdmCl-denatured (◆) and GdmCl-denatured-reduced (×) states. The HEWL and RNase A data have been scaled to the same water/protein mole ratio (N_T = 28,500) as used for BαLA. The curves represent fits according to equation 1. Solution conditions and fitted hydration parameters are given in Table 1.

relative dynamic retardation ρ_α in the range 3.9–4.4, as for other small proteins[27].

To elucidate the molecular basis of the dynamic retardation factor ρ_α for native and nonnative proteins, we measured the water ^{17}O relaxation rate in aqueous amino acid mixtures (pH* 1.2–1.6, 27 °C) of the same composition and concentration as in the investigated BαLA and RNase A solutions. As expected, the relaxation rate was independent of frequency (data not shown). We thus obtained $N_\alpha\rho_\alpha$ = 1470 ± 100 per 'protein' for both BαLA and RNase A. Since the difference in ρ_α between free and polymerized amino acids is <10% (ref. 30), this result can be taken as a reference value for a fully solvated polypeptide chain of ~120 residues. With N_α estimated as described above, we obtain ρ_α = 1.3 ± 0.1, in accord with a previous ^{17}O relaxation study of amino acid solutions[30]. The larger dynamic retardation factor, $\rho_\alpha \approx 4$, at the surface of native proteins is probably dominated by a minority ($<<N_\alpha$) of water sites with concave (groove) geometry and good hydrogen-bonding possibilities. (One third of the water molecules at protein surfaces in crystals make two or more hydrogen bonds to protein atoms[31].)

Hydration of proteins denatured by GdmCl

The complete unfolding of a native globular protein into a solvent-exposed polypeptide coil should be strongly manifested in the MRD profile. The relaxation dispersion should vanish, since all cavities and pockets containing long-lived water molecules are disrupted. The net effect on the high-frequency plateau ($N_\alpha\rho_\alpha$) is less obvious. On the one hand, N_α should increase by as much as a factor of three as a result of the larger solvent-accessible area of the unfolded polypeptide chain. On the other hand, the loss of surface sites with strong dynamic retardation should decrease ρ_α by a similar factor. Both of these trends will be modified by the presence of denaturant at high concentration in the bulk solvent and at the polypeptide surface.

As predicted, the relaxation dispersion has vanished for BαLA, HEWL and RNase A in the DR state, that is, denatured by high GdmCl concentration and with the disulfide bonds reduced by dithiothreitol (Fig. 2). For all three proteins, however, a small but significant dispersion step remains in the D state, that is, when the disulfide bonds are intact (Fig. 2). This dispersion can be accounted for by a single, moderately ordered water molecule trapped in a small region with persistent structure, presumably near one of the disulfide bonds (and not necessarily related to any of the long-lived sites in the N state). The residence time of this water molecule would have to be longer than τ_β (~5 ns) and shorter than $(\omega_Q^2 S_\beta^2 \tau_R)^{-1} \approx$ 5–10 μs[25]. Alternatively, the small dispersion step from the disulfide-intact D state could be produced by a larger number of weakly ordered water molecules that remain within a constrained region for >5 ns.

If disulfide reduction leads to further unfolding of the polypeptide chain, it should also affect the hydration parameter $N_\alpha\rho_\alpha$ that determines the high-frequency plateau of the MRD profile. This is the case for RNase A, but not for the homologous BαLA and HEWL (Fig. 2). Since the MRD profiles from the denatured forms of BαLA and RNase A refer to similar GdmCl concentrations (4.4 and 4.0 M), they can be compared directly. The data in Fig. 2 thus indicate that the DR states of these two proteins have nearly the same solvent exposure. When HEWL and BαLA are studied at the same GdmCl concentration (7.0 M), nearly identical MRD profiles are obtained for the denatured states. The smaller relaxation enhancement for HEWL seen in Fig. 2 is a result of competitive solvation, with more surface water being displaced at the higher GdmCl concentration (see below). Even without a detailed analysis of competitive solvation, we can conclude that the DR states of the three investigated proteins are very similar with respect to hydration ($N_\alpha\rho_\alpha$) and, therefore, are likely to have similar configurational statistics. The homologous BαLA and HEWL also have very similar D states, whereas the smaller relaxation enhancement for RNase A shows that the hydration of its D state is less extensive (smaller N_α) or less dynamically perturbed (smaller ρ_α). This is consistent with reports of substantial residual helix content and aromatic side-chain clustering in GdmCl-denatured RNase A[1,3,32].

To analyze quantitatively MRD data from solvent-denatured proteins, we must recognize that GdmCl not only unfolds the protein but also competes with water for solvation sites. To disentangle these effects, we recorded ^{17}O MRD profiles for BαLA at several GdmCl concentrations. The hydration parameters $N_\alpha\rho_\alpha$ and $N_\beta S_\beta^2$ derived from these profiles (Fig. 3) are well described by a two-state N → D transition with the free-energy difference decreasing linearly with GdmCl concentration[33]. The coincidence of the $N_\alpha\rho_\alpha$ and $N_\beta S_\beta^2$ transitions (Fig. 3) shows that the release of the long-lived internal water molecules present in the N state occurs in the same cooperative unfolding event as the influx of short-lived water molecules into the expanded D state. The apparent two-state behavior also shows that the MG intermediate, which is maximally populated at GdmCl concentrations of 2–3 M (ref. 5), cannot have a much larger number (N_β) of long-lived (internal) water molecules than the N state. A fit to the combined $N_\alpha\rho_\alpha$ and $N_\beta S_\beta^2$ data yields a midpoint concentration, $c_{1/2}$, of 2.6 ± 0.2 M and an m value of 4.8 ± 1.7 kJ mol^{-1} M^{-1}. The close agreement of these values with those derived from the far-UV CD curve[34] suggests that the major hydration changes on GdmCl denaturation are correlated with the disruption of secondary structure.

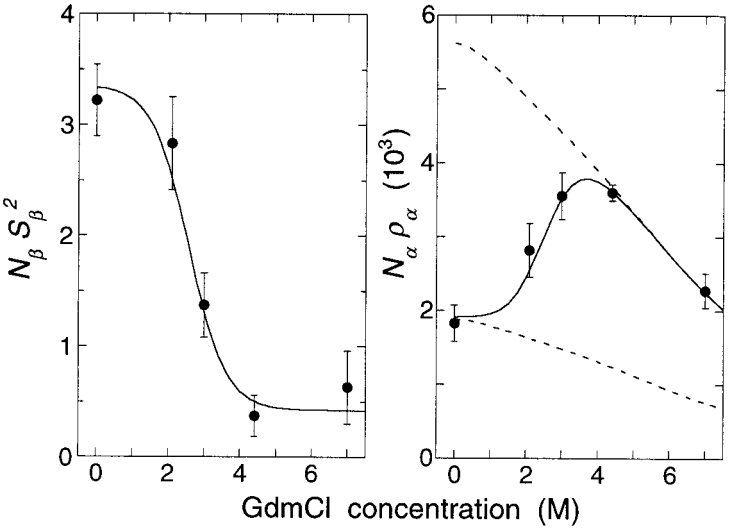

Fig. 3 Variation with GdmCl concentration of the hydration parameters $N_\beta S_\beta^2$ (left) and $N_\alpha \rho_\alpha$ (right) derived from ^{17}O MRD profiles from α-lactalbumin solutions. The solid curves resulted from a fit of equations 2 and 3 to the combined $N_\beta S_\beta^2$ and $N_\alpha \rho_\alpha$ data. The dashed curves show the effect of displacement of surface water by GdmCl on $N_\alpha \rho_\alpha$ for the D and N states .

According to the analysis of the GdmCl denaturation data in Fig. 3, the reduction of $N_\alpha \rho_\alpha$ above the unfolding transition is due to the gradual replacement of water by GdmCl at the surface of the denatured protein. This effect was modeled (see Methods) as a weak binding of GdmCl at independent sites[35,36], and the fit in Fig. 3 gave an average GdmCl-binding constant (for the D state) $K_b = 0.16 \pm 0.07\ M^{-1}$, in good agreement with calorimetrically determined K_b values for HEWL and RNase A[37,38]. This analysis allows us to extract from the fit an intrinsic hydration parameter, $[N_\alpha \rho_\alpha]_D = 5{,}600 \pm 900$, for the D state in the absence of GdmCl competition (see the dashed curve in Fig. 3). Since this value is a factor of 3.8 larger than for a fully hydrated polypeptide chain, as estimated from measurements on amino acid mixtures, we conclude that the D-state hydration is much more dynamically perturbed (by at least a factor of four in ρ_α) than water in contact with a fully exposed polypeptide chain. This suggests that a substantial fraction of the water molecules that penetrate the denatured protein interact strongly with several polypeptide segments and, therefore, that the structure of the D state contains relatively compact domains. This view is consistent with the presence of a collapsed core in α-lactalbumin at high urea concentrations[39]. The finding that $N_\alpha \rho_\alpha$ is unaffected by reduction of the four disulfide bonds in BαLA and HEWL (Fig. 2) implies that the compact domains are not due to topological constraints, although the loss of the residual dispersion suggests that these domains become more dynamic. While these qualitative conclusions about the nature of the D state follow rather directly from the data, the quantitative inferences rely on several assumptions and are therefore less firm. In particular, the deduced value of $[N_\alpha \rho_\alpha]_D$ relies heavily on the accuracy of the two points (4.4 and 7.0 M) above the unfolding transition, on the validity of the weak-binding model, and on the assumption that neither the configurational statistics of the polypeptide chain nor the dynamic retardation factor ρ_α (which is defined with respect to the bulk solvent) vary with the GdmCl concentration in this range.

Hydration of molten globule proteins

According to the prevalent view, the N → MG transition is accompanied by an influx of hundreds of water molecules[5,7,8,17–22]. If this is correct, a drastic change of the MRD profile is expected. The dispersion step would vanish if the water molecules buried in the native structure become accessible and therefore short-lived. On the other hand, if some of the penetrating water molecules are long-lived ($\tau_W > 1$ ns) and at least moderately ordered, the dispersion step would increase markedly. The high-frequency relaxation enhancement ($N_\alpha \rho_\alpha$) is expected to increase, since most of the hundreds of penetrating water molecules should be strongly retarded in their rotational dynamics (even more so than in the GdmCl-induced D state).

The ^{17}O MRD profiles from BαLA, apoMb and HCAII in their N and acid-induced MG states are compared in Fig. 4, which also includes MRD profiles from acid-denatured apoMb and GdmCl-denatured HCAII. The results for the MG proteins are noteworthy in two respects. First, the MG state yields a sizeable dispersion, comparable in magnitude to that of the N state. Second, the high-frequency relaxation enhancement is nearly the same for the N and MG states. As argued below, both of these observations seem to be inconsistent with a major solvent penetration of the MG.

For the native proteins, the magnitude of the dispersion step, $N_\beta S_\beta^2 = 3.2$, 1.5 and 8.1 for BαLA, apoMb and HCAII, correlates well with the number of potentially long-lived water molecules ($N_\beta = 6$, 2, and ~20, respectively) in crystal structures (PDB files 1HML, 1HRM and 2CBA, respectively). In native BαLA, the Ca^{2+} ion coordinates two (probably long-lived[29]) water molecules and resides in the same cavity (between the α- and β-subdomains) as three additional potentially long-lived water molecules (Fig. 1). The 50% reduction of $N_\beta S_\beta^2$ can therefore be largely attributed to the loss of Ca^{2+} affinity in the MG state[40,41]. Several studies have indicated that the α-lactalbumin MG at pH 2 has a bipartite structure with an expanded α-domain with native-like tertiary fold and a predominantly unfolded β-domain[10,42]. Since there are no internal water molecules within the native α-domain (Fig. 1), the two or more ($N_\beta S_\beta^2 = 1.6$) long-lived water molecules in the MG state might be unrelated to the native internal water molecules.

Native apomyoglobin has the smallest internal hydration among the five proteins investigated here (Table 1). Native myoglobin has an exceptionally loose packing, with internal cavities (280 Å^3 in holoMb[27]) that appear to be empty in crystal structures. For holoMb, a previous MRD study[27] gave $N_\beta S_\beta^2 = 2.3 \pm 0.2$, slightly more than found here for apoMb, but the location of the responsible internal water molecules has not been established. According to ^1H and ^{13}C NMR, the structure of native apoMb closely resembles native holoMb, except for the disordered F helix near the empty heme pocket[43,44]. Also the MG state of apoMb is highly structured, with essentially intact A, B, G and H helices[44], whereas the acid-denatured state (pH 2.3) retains significant (20–35%) helicity only in helices A, D and H[44]. Unless our 2 mM sample of acid-denatured (pH* 2.2) apoMb contains a substantial fraction (~40%) of MG state, the small but significant dispersion observed for this sample (Fig. 4) implies that the residual structure in the D state is able to trap at least one long-lived water molecule. In contrast to the GdmCl-denatured proteins, acid-denatured apoMb has a smaller high-frequency

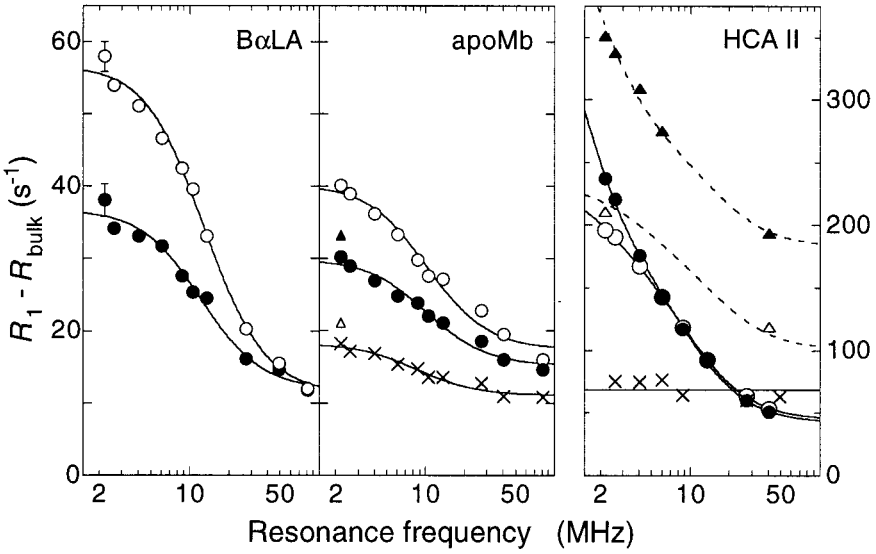

Fig. 4 Frequency dependence of water ^{17}O excess longitudinal relaxation rate from solutions of α-lactalbumin, apomyoglobin and carbonic anhydrase II in the native (○) and molten globule (●) states, and from solutions of acid-denatured apoMb (×) and GdmCl-denatured HCAII (×). Transverse relaxation data are also shown for the N and MG states (△,▲) of HCAII and for the D and MG states (△,▲) of apoMb. The apoMb and HCAII data have been scaled to the same water/protein mole ratio (N_T = 28,500) as used for BαLA. The curves represent fits according to equation 1, except for HCAII, where a bilorentzian fit to the combined longitudinal and transverse relaxation data was performed. Solution conditions and fitted hydration parameters are given in Table 1.

relaxation enhancement than the N state (Fig. 4). The $N_\alpha\rho_\alpha$ value obtained for the acid-denatured state is consistent with a fully hydrated polypeptide chain, with ρ_α estimated from measurements on amino acid mixtures. The apoMb MG dispersion, however, is closer to the N state with respect to both $N_\alpha\rho_\alpha$ and $N_\beta S_\beta^2$ (Fig. 4, Table 1). The dispersion step can be accounted for by one or two long-lived water molecules, possibly corresponding to (but less ordered than) those in native apoMb. The apoMb sample had a very high viscosity, which was markedly reduced on acid denaturation (pH* 2.2). This large variation in macroscopic viscosity was not reflected in the correlation time τ_β (Table 1).

For HCAII and the homologous bovine carbonic anhydrase B, acid (pH 3–4)- and GdmCl (1–2 M)-induced MG states have been identified[5,45,46]. The latter has a native-like β-sheet structure in the central part, and a large associated hydrophobic cluster remains stable even at high GdmCl concentrations[45,46]. The MRD data (Fig. 4) show that HCAII denatured in 4 M GdmCl is devoid of long-lived water molecules. For the N and MG states of HCAII, the absence of a low-frequency plateau in the MRD profiles indicates some protein association. Transverse relaxation data, which are more sensitive to slow motions (rotational diffusion of protein oligomers), show that association is more pronounced for the MG (Fig. 4). The reported hydration parameters (Table 1) are population-weighted averages obtained from a bilorentzian fit to the combined longitudinal and transverse MRD data. (Since the average $N_\beta S_\beta^2$ is proportional to the integral of the dispersion curve, it is hardly affected by the low-frequency data[47].) The near invariance of $N_\beta S_\beta^2$ under the N → MG transition (Table 1) indicates a high degree of correspondence between the long-lived water molecules in the two states, suggesting that the MG has a predominantly native-like and persistent (>10 ns) structure.

The striking convergence of the MRD profiles from the N and MG states at high frequency (Fig. 4) implies that, for all three proteins, the external (short-lived) hydration is similar for these states. The ratio $N_\alpha\rho_\alpha$ (MG) / $N_\alpha\rho_\alpha$ (N) is 1.1 ± 0.1 for BαLA, 0.9 ± 0.1 for apoMb and 1.0 ± 0.1 for HCAII, which may be compared with $N_\alpha\rho_\alpha$ (D) / $N_\alpha\rho_\alpha$ (N) = 0.64 ± 0.06 for acid-denatured apoMb. From the $N_\alpha\rho_\alpha$ values (Table 1) and hydration numbers estimated from the solvent-accessible areas of the native proteins (N_α = 470, 550 and 780 for BαLA, apoMb and HCAII), we obtain for the relative dynamic retardation ρ_α = 3.9, 5.1 and 9.0, respectively. The larger value for HCAII is attributed to the abundance of hydrated surface pockets (seen in the crystal structure) and to slow internal motion of some of the ~20 potentially long-lived internal water molecules (as previously suggested for trypsin[27]). The large variation in (native) structure among the three proteins strongly suggests that the near equality of $N_\alpha\rho_\alpha$ for the N and MG states is not accidental (increased N_α compensated by decreased ρ_α). We therefore conclude that the external hydration of the investigated MG proteins differs little from that of the corresponding native proteins, both in its extent (N_α) and in its dynamics (ρ_α). Since ρ_α for the N state appears to be dominated by strongly interacting surface water molecules in grooves (see above), the present results suggest that most of these hydration sites are preserved in the MG state.

Implications for protein stability and folding

The present MRD data on GdmCl-denatured proteins show that loss of specific internal water sites and influx of external solvent are concomitant with disintegration of secondary structure (as seen by CD). This is consistent with the view that disruption of α-helices and β-sheets is promoted by water acting as a competitive hydrogen bond partner[48]. The large dynamic retardation inferred for the D state suggests that water penetrating the GdmCl-denatured protein differs substantially from the hydration shell of a fully exposed polypeptide chain. Taken together with the residual dispersion from the D state of all three investigated proteins, this suggests that even strongly solvent-denatured proteins contain relatively compact domains. This is consistent with the finding that mutations can exert their destabilizing effects directly on the denatured state[6,9]. Furthermore, for BαLA and HEWL, disulfide bond cleavage appears to affect the flexibility of the denatured protein more than its average structure. Our data thus suggest that, even under extremely denaturing conditions (such as 7 M GdmCl + DDT), proteins are far from the idealized random-coil state.

The conclusion from the present water ^{17}O MRD study that the molten globule states of three structurally unrelated proteins closely resemble the native proteins with regard to internal hydration and surface topography contrasts with the picture of a highly water-penetrated MG inferred from several other (less

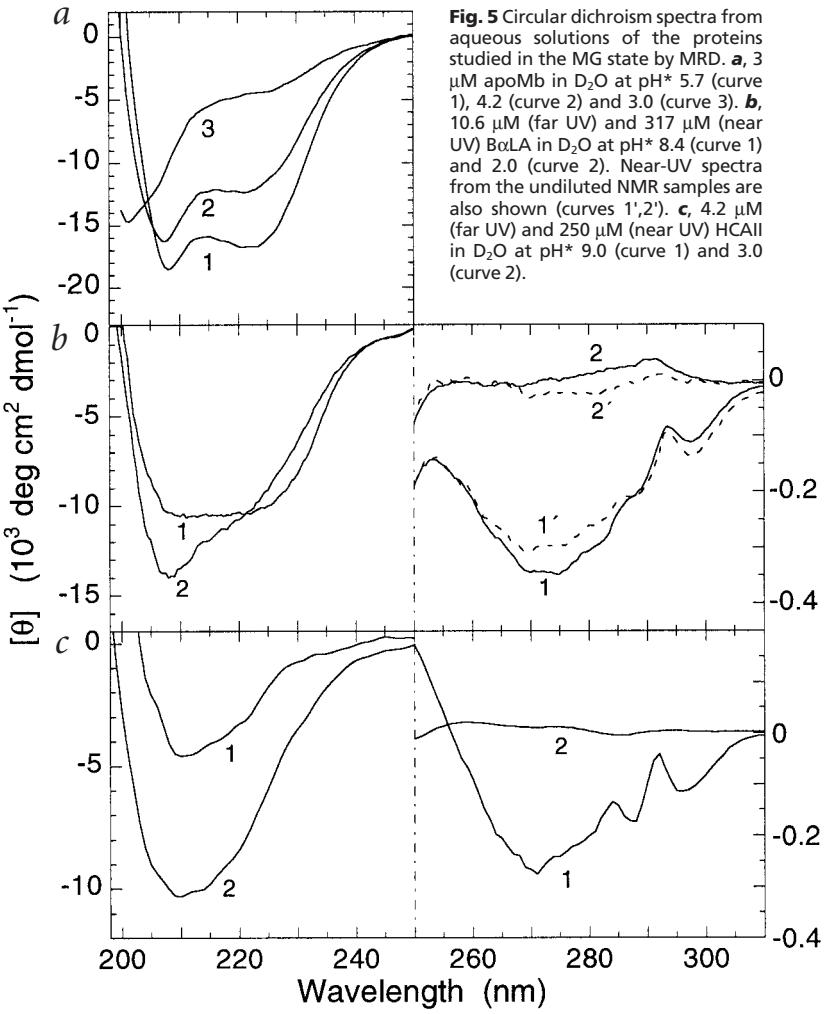

Fig. 5 Circular dichroism spectra from aqueous solutions of the proteins studied in the MG state by MRD. ***a***, 3 μM apoMb in D_2O at pH* 5.7 (curve 1), 4.2 (curve 2) and 3.0 (curve 3). ***b***, 10.6 μM (far UV) and 317 μM (near UV) BαLA in D_2O at pH* 8.4 (curve 1) and 2.0 (curve 2). Near-UV spectra from the undiluted NMR samples are also shown (curves 1',2'). ***c***, 4.2 μM (far UV) and 250 μM (near UV) HCAII in D_2O at pH* 9.0 (curve 1) and 3.0 (curve 2).

direct) studies. Scattering measurements that probe the compactness of the MG state suggest that its volume is at least 30% larger than for the N state[13–16]. It has been argued that a large amount of water must therefore be incorporated into the MG[5,7,8,17–22]. A 30% volume expansion of a 14 kDa protein corresponds to ~5000 Å^3, or 200 water molecules (with 24 Å^3 molecule^{-1}; ref. 31). Such a massive influx of water into the MG structure is incompatible with the present MRD data, since it would substantially alter the hydration parameters $N_\alpha\rho_\alpha$ and $N_\beta S_\beta$[2]. According to the MRD data in Fig. 4, the hydration parameter $N_\alpha\rho_\alpha$ is nearly invariant under the N → MG transition. Since $N_\alpha\rho_\alpha$ is known to vary greatly with protein size (mainly through N_α) and with surface structure ($\rho_\alpha \approx 4$ for a native protein surface versus $\rho_\alpha = 1.3$ for a fully hydrated polypeptide chain), a major change in hydration at the N → MG transition would have been clearly seen in the MRD data. The present MRD results thus call for a reinterpretation of the small-angle scattering data that does not invoke solvent penetration of the MG. According to diffuse X-ray scattering, side-chain disorder can increase the volume of the MG by ~10%[49] without creating cavities large enough to accommodate water[40]. Furthermore, the radius of gyration and the hydrodynamic radius could be affected by local unfolding and conformational heterogeneity at levels that would not significantly affect the MRD hydration parameters.

Another argument for strongly enhanced hydration of the MG is based on the insignificant heat capacity difference between the MG and D states[2,5,50]. More recent calorimetric data, however, indicate that the heat capacity change for the N → MG transition is comparable to[7,50], or even less than[51], that for the MG → D transition. On the premise that heat capacity differences are due mainly to exposure of hydrophobic side chains, this nevertheless implies a substantial water penetration of the MG[7]. This premise is based on calorimetric data for bulk solution transfer of small molecules and may not be quantitatively valid if the properties of water inside denatured proteins differ markedly from the hydration shell of a solute immersed in bulk water. Furthermore, there may well be other significant contributions to the heat capacity difference[52,53].

A growing body of evidence suggests that equilibrium MG states are closely related to early kinetic intermediates on the folding pathway[2,4–8,54–57]. Our finding that the internal and external hydration of the MG differ little from the N state therefore has implications for the folding mechanism. In particular, the presence of much of the native internal hydration in the MG suggests that these specific water molecules, which may be viewed as an extension of the secondary structure, are in place before the native tertiary structure is fully formed. Conversely, the exchange of these buried water molecules with bulk water under native conditions must involve excited conformational substates that are more unfolded than the MG. The time scale for this exchange is generally in the range 10 ns to 1 ms at room temperature[24,25,27]. (For one of the buried water molecules in BPTI, the exchange time is accurately known[28]: 170 ± 20 μs at 27 °C). It thus appears that native proteins access MG-like states by thermal fluctuations on a submillisecond time scale. Temperature-dependent MRD studies of MG proteins may shed further light on the mechanism and dynamics of unfolding.

Methods

Sample preparation. Bovine α-lactalbumin (type I), hen egg-white lysozyme (L 6876), bovine pancreatic ribonuclease A (type XII-A) and myoglobin from horse skeletal muscle (M 0630) were purchased from Sigma as lyophilized powders. Recombinant human carbonic anhydrase II was expressed and purified as described[58]. Apomyoglobin was prepared from myoglobin by acid 2-butanone extraction[59], followed by extensive dialysis against pure water at 8 °C. α-Lactalbumin was dialyzed against pure water and RNase A was purified by chromatography as described[26], with subsequent lyophilization for all proteins. Protein solutions were made from pure D_2O enriched to 21.9 atom% ^{17}O (Ventron). The desired pH* value (quoted without H/D isotope correction) was obtained by minute additions of 1 M HCl or NaOH. For HCAII, small amounts of 0.1 M NaOH, H_2SO_4 and $ZnSO_4$ were added before lyophilization. For all proteins, the reported pH* values were measured directly in the NMR tube. Protein concentrations were determined from the optical absorption (after 60-fold dilution in 6 M GdmCl, 20 mM phosphate, pH 6.5), using calculated extinction coefficients[32].

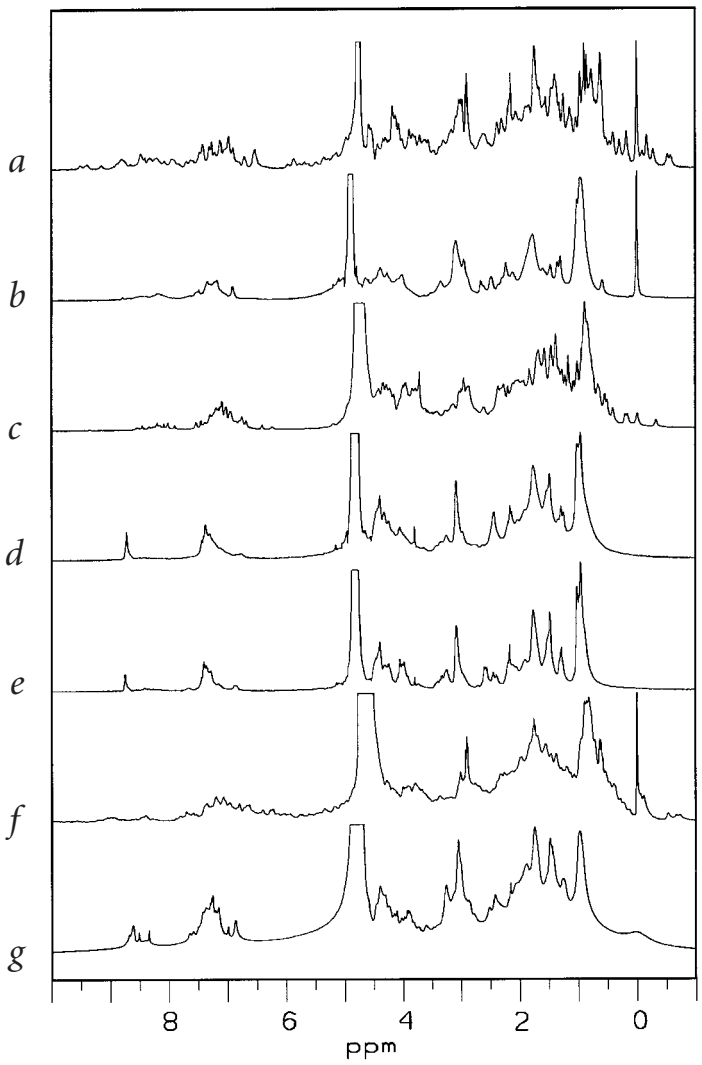

Fig. 6 ^{1}H NMR spectra from aqueous solutions of the proteins studied in the MG state by MRD: ***a***, BαLA (N), ***b***, BαLA (MG), ***c***, apoMb (N), ***d***, apoMb (MG), ***e***, apoMb (D), ***f***, HCAII (N), and ***g***, HCAII (MG). Solution conditions are the same as for the MRD samples (Table 1). Chemical shifts are referenced relative to DSS.

Guanidinium chloride (ultrapure) was purchased from U.S. Biochemical and dithiothreitol (>97%) from Wako. Disulfide reduction was performed (after GdmCl denaturation) directly in the NMR samples by addition of 100 mM dithiothreitol and incubation at room temperature and neutral pH for at least 1 h.

The presence of the MG state in our MRD samples was verified by CD spectra (Fig. 5), recorded at 27 °C on a JASCO J-720 spectropolarimeter, and by high-resolution ^{1}H NMR spectra, recorded at 27 °C on a GE Omega 500 MHz spectrometer. For the CD measurements, the MRD samples were diluted [(180–600)-fold and (3–10)-fold for the far- and near-UV spectral regions, respectively]. The dilution was done with D_2O adjusted to the pH* of the protein solution with HCl, after which pH* was measured again. Wavelength scans were performed with 0.5 nm resolution using 1 mm optical cells. For the apoMb and BαLA MGs, our CD spectra (Fig. 5*a*,*b*) are very similar to those reported in the literature[34,40,60,61], and for HCAII they closely resemble the ones reported for the MG state induced by 1.5 M GdmCl[45] and for the MG state of the homologous bovine enzyme at pH* 3.0 [62,63]. Near-UV CD spectra from the undiluted NMR samples of BαLA, recorded with a 0.1 mm optical cell, were similar to the ones recorded after sixfold dilution (Fig. 5*b*). The ^{1}H NMR spectra were recorded with the actual MRD samples (apoMb) or with subsequently prepared replicas of the MRD samples (BαLA and HCAII). These spectra (Fig. 6) are closely similar to the ones reported in the literature[40,64,65]. In particular, the upfield methyl resonances are absent from the MG spectra of all three proteins.

Magnetic relaxation dispersion (MRD) measurements. The ^{17}O longitudinal relaxation rates, R_1, of the water resonance was measured as described[66] at magnetic fields in the range 0.38–14.1 T, using three Bruker and three Varian NMR spectrometers and a Drusch EAR-35N iron magnet. The relaxation rate, R_{bulk}, of the bulk solvent at different GdmCl concentrations was also measured, using water with the same solvent isotope composition as in the protein solutions. All measurements were done at 27.0 ± 0.1 °C. The MRD data, that is, R_1 as a function of the resonance frequency ω_0, were analyzed with the theoretical expression[25,27]

$$R_1 - R_{bulk} = \alpha + \beta[0.2\, j(\omega_0) + 0.8\, j(2\omega_0)] \qquad (1)$$

with a lorentzian spectral density function $j(\omega) = \tau_\beta / [1 + (\omega\tau_\beta)^2]$. The three parameters α, β and τ_β were determined from a nonlinear fit and converted to molecular hydration parameters according to $N_\alpha\rho_\alpha = \alpha N_T / R_{bulk}$ and $N_\beta S_\beta^2 = \beta N_T / \omega_Q^2$, with N_T the water/protein mole ratio and $\omega_Q = 7.61 \times 10^6$ rad s^{-1} the ^{17}O (rigid-lattice) quadrupole frequency[25].

In the GdmCl titration experiments, the hydration parameters ($P = N_\alpha\rho_\alpha$ or $N_\beta S_\beta^2$) obtained from the dispersion fit were assumed to be exchange averaged according to

$$P = f_N P_N + (1 - f_N) P_D \qquad (2)$$

The fraction native protein was expressed as $f_N = 1 / (1 + K_D)$, with the denaturation constant given by[33]

$$K_D = \exp[m(c - c_{1/2}) / (RT)] \qquad (3)$$

Competitive solvent binding was taken into account by multiplying $[N_\alpha\rho_\alpha]_N$ and $[N_\alpha\rho_\alpha]_D$ by the factor $[1 - K_b a / (a_W + K_b a)]$, with the GdmCl activity a (molarity scale) and water activity a_W (mole fraction scale) taken from the literature[33,35]. By adopting this solvent exchange model[35,36], we attribute the direct effect of GdmCl on $N_\alpha\rho_\alpha$ (at fixed protein conformation) to N_α, neglecting any variation in ρ_α due to a difference in the GdmCl-induced perturbation of water dynamics between the solvation layer and the bulk solvent. Since R_{bulk} (proportional to τ_{bulk}) increases by merely 30% from 0 to 7 M GdmCl, and since ρ_α involves the ratio $\tau_\alpha / \tau_{bulk}$, the dynamic effect should be negligible compared to the threefold variation of $N_\alpha\rho_\alpha$ due to protein unfolding. Moreover, linear extrapolation from the two highest GdmCl concentrations yields essentially the same $[N_\alpha\rho_\alpha]_D$ as the fit based on the solvent exchange model. Since any ρ_α variation should be linear, it would only affect the apparent binding constant K_b.

The solvent-accessible area of unfolded proteins was taken from the literature[67].

Acknowledgments

We thank E. Thulin for help with protein purification. This work was supported by the Swedish Natural Science Research Council (NFR) and the Royal Swedish Academy of Sciences (KVA).

Received 6 October, 1998; accepted 11 November, 1998.

1. Tanford, C. Protein denaturation. *Adv. Protein Chem.* **23**, 121–282 (1968).
2. Kuwajima, K. The molten globule state as a clue for understanding the folding and cooperativity of globular-protein structure. *Proteins* **6**, 87–103 (1989).
3. Dill, K.A. & Shortle, D. Denatured states of proteins. *Annu. Rev. Biochem.* **60**, 795–825 (1991).
4. Dobson, C.M. Unfolded proteins, compact states and molten globules. *Curr. Opin. Struct. Biol.* **2**, 6–12 (1992).
5. Ptitsyn, O.B. in *Protein folding* (ed. Creighton, T.E.) 243–300 (W.H. Freeman & Co., New York; 1992).
6. Shortle, D. Denatured states of proteins and their roles in folding and stability. *Curr. Opin. Struct. Biol.* **3**, 66–74 (1993).
7. Freire, E. Thermodynamics of partly folded intermediates in proteins. *Annu. Rev. Biophys. Biomol. Struct.* **24**, 141–165 (1995).
8. Fink, A.L. Compact intermediate states in protein folding. *Annu. Rev. Biophys. Biomol. Struct.* **24**, 495–522 (1995).
9. Shortle, D. The denatured state (the other half of the folding equation) and its role in protein stability. *FASEB J.* **10**, 27–34 (1996).
10. Kuwajima, K. The molten globule state of α-lactalbumin. *FASEB J.* **10**, 102–109 (1996).
11. Spolar, R.S., Livingstone, J.R. & Record, M.T. Use of liquid hydrocarbon and amide transfer data to estimate contributions to thermodynamic functions of protein folding from the removal of nonpolar and polar surface from water. *Biochemistry* **31**, 3947–3955 (1992).
12. Makhatadze, G.I. & Privalov, P.L. Hydration effects in protein unfolding. *Biophys. Chem.* **51**, 291–309 (1994).
13. Gast, K., Zirwer, D., Welfle, H., Bychkova, V.E. & Ptitsyn, O.B. Quasielastic light scattering from human α-lactalbumin: comparison of molecular dimensions in native and molten globule states. *Int. J. Biol. Macromol.* **8**, 231–236 (1986).
14. Kataoka, M., Kuwajima, K., Tokunaga, F. & Goto, Y. Structural characterization of the molten globule of α-lactalbumin by solution X-ray scattering. *Protein Sci.* **6**, 422–430 (1997).
15. Gast, K. *et al.* Compactness of protein molten globules: temperature-induced structural changes of the apomyoglobin folding intermediate. *Eur. Biophys. J.* **23**, 297–305 (1994).
16. Kataoka, M. *et al.* Structural characterization of the molten globule and native states of apomyoglobin by solution X-ray scattering. *J. Mol. Biol.* **249**, 215–228 (1995).
17. Nishii, I., Kataoka, M., Tokunaga, F. & Goto, Y. Cold denaturation of the molten globule states of apomyoglobin and a profile for protein folding. *Biochemistry* **33**, 4903–4909 (1994).
18. Uchiyama, H., Perez-Prat, E.M., Watanabe, K., Kumagai, I. & Kuwajima, K. Effects of amino acid substitutions in the hydrophobic core of α-lactalbumin on the stability of the molten globule state. *Protein Eng.* **8**, 1153–1161 (1995).
19. Kharakoz, D.P. & Bychkova, V.E. Molten globule of human α-lactalbumin: hydration, density, and compressibility of the interior. *Biochemistry* **36**, 1882–1890 (1997).
20. Finkelstein, A.V. & Shakhnovich, E.I. Theory of cooperative transitions in protein molecules. II. Phase diagram for a protein molecule in solution. *Biopolymers* **28**, 1681–1694 (1989).
21. Alonso, D.O.V., Dill, K.A. & Stigter, D. The three states of globular proteins: acid denaturation. *Biopolymers* **31**, 1631–1649 (1991).
22. Williams, M.A., Thornton, J.M. & Goodfellow, J.M. Modelling protein unfolding: hen egg-white lysozyme. *Protein Eng.* **10**, 895–903 (1997).
23. Kunz, I.D. & Kauzmann, W. Hydration of proteins and polypeptides. *Adv. Protein Chem.* **28**, 239–345 (1974).
24. Otting, G. NMR studies of water bound to biological molecules. *Prog. NMR Spectrosc.* **31**, 259–285 (1997).
25. Halle, B., Denisov, V.P. & Venu, K. in *Modern techniques in protein NMR* Vol. 17 (eds Berliner, L.J. & Krishna, N.R.) **in the press** (Plenum Press, New York; 1999).
26. Denisov, V.P. & Halle, B. Thermal denaturation of ribonuclease A characterized by water ^{17}O and ^{2}H magnetic relaxation dispersion. *Biochemistry* **37**, 9595–9604 (1998).
27. Denisov, V.P. & Halle, B. Protein hydration dynamics in aqueous solution. *Faraday Discuss.* **103**, 227–244 (1996).
28. Denisov, V.P., Peters, J., Hörlein, H.D. & Halle, B. Using buried water molecules to explore the energy landscape of proteins. *Nature Struct. Biol.* **3**, 505–509 (1996).
29. Denisov, V.P. & Halle, B. Direct observation of calcium-coordinated water in calbindin D_{9k} by nuclear magnetic relaxation dispersion. *J. Am. Chem. Soc.* **117**, 8456–8465 (1995).
30. Ishimura, M. & Uedaira, H. Natural-abundance oxygen-17 magnetic relaxation in aqueous solutions of apolar amino acids and glycine peptides. *Bull Chem. Soc. Jpn.* **63**, 1–5 (1990).
31. Gerstein, M. & Chothia, C. Packing at the protein-water interface. *Proc. Natl. Acad. Sci. USA* **93**, 10167–10172 (1996).
32. Edelhoch, H. Spectroscopic determination of tryptophan and tyrosine in proteins. *Biochemistry* **6**, 1948–1954 (1967).
33. Pace, C.N. Determination and analysis of urea and guanidine hydrochloride denaturation curves. *Methods Enzymol.* **131**, 266–280 (1986).
34. Kuwajima, K., Nitta, K., Yoneyama, M. & Sugai, S. Three-state denaturation of α-lactalbumin by guanidine hydrochloride. *J. Mol. Biol.* **106**, 359–373 (1976).
35. Schellman, J.A. The thermodynamics of solvent exchange. *Biopolymers* **34**, 1015–1026 (1994).
36. Schellman, J.A. A simple model for solvation in mixed solvents. Application to the stabilization and destabilization of macromolecular structures. *Biophys. Chem.* **37**, 121–140 (1990).
37. Makhatadze, G.I. & Privalov, P.L. Protein interactions with urea and guanidinium chloride. A calorimetric study. *J. Mol. Biol.* **226**, 491–505 (1992).
38. Schellman, J.A. & Gassner, N.C. The enthalpy of transfer of unfolded proteins into solutions of urea and guanidinium chloride. *Biophys. Chem.* **59**, 259–275 (1996).
39. Schulman, B.A., Kim, P.S., Dobson, C.M. & Redfield, C. A residue-specific NMR view of the non-cooperative unfolding of a molten globule. *Nature Struct. Biol.* **4**, 630–634 (1997).
40. Dolgikh, D.A. *et al.* Compact state of a protein molecule with pronounced small-scale mobility: bovine α-lactalbumin. *Eur. Biophys. J.* **13**, 109–121 (1985).
41. Kronman, M.J. Metal-ion binding and the molecular conformational properties of α-lactalbumin. *Crit. Rev. Biochem. Mol. Biol.* **24**, 565–667 (1989).
42. Wu, L.C., Peng, Z. & Kim, P.S. Bipartite structure of the α-lactalbumin molten globule. *Nature Struct. Biol.* **2**, 281–286 (1995).
43. Lecomte, J.T.J., Kao, Y.H. & Cocco, M.J. The native state of apomyoglobin described by proton NMR spectroscopy: the A-B-G-H interface of wild-type sperm whale apomyoglobin. *Proteins* **25**, 267–285 (1996).
44. Eliezer, D., Yao, J., Dyson, H.J. & Wright, P.E. Structural and dynamic characterization of partially folded states of apomyoglobin and implications for protein folding. *Nature Struct. Biol.* **5**, 148–155 (1998).
45. Mårtenson, L.-G. *et al.* Characterization of folding intermediates of human carbonic anhydrase II: Probing substructure by chemical labeling of SH groups introduced by site-directed mutagenesis. *Biochemistry* **32**, 224–231 (1993).
46. Svensson, M. *et al.* Mapping the folding intermediate of human carbonic anhydrase II. Probing substructure by chemical reactivity and spin and fluorescence labeling of engineered cysteine residues. *Biochemistry* **34**, 8606–8620 (1995).
47. Halle, B., Jóhannesson, H. & Venu, K. Model-free analysis of stretched relaxation dispersions. *J. Magn. Reson.* **135**, 1–13 (1998).
48. Barron, L.D., Hecht, L. & Wilson, G. The lubricant of life: a proposal that solvent water promotes extremely fast conformational fluctuations in mobile heteropolypeptide structure. *Biochemistry* **36**, 13143–13147 (1997).
49. Damaschun, G., Gernat, C., Damaschun, H., Bychkova, V.E. & Ptitsyn, O.B. Comparison of intramolecular packing of a protein in native and 'molten globule' states. *Int. J. Biol. Macromol.* **8**, 226–230 (1986).
50. Pfeil, W. Is the molten globule a third thermodynamic state of protein? The example of α-lactalbumin. *Proteins* **30**, 43–48 (1998).
51. Griko, Y.V. & Privalov, P.L. Thermodynamic puzzle of apomyoglobin unfolding. *J. Mol. Biol.* **235**, 1318–1325 (1994).
52. Hinz, H.-J., Vogl, T. & Meyer, R. An alternative interpretation of the heat capacity changes associated with protein unfolding. *Biophys. Chem.* **52**, 275–285 (1994).
53. Yang, D., Mok, Y.-K., Forman-Kay, J.D., Farrow, N.A. & Kay, L.E. Contributions to protein entropy and heat capacity from bond vector motions measured by NMR spin relaxation. *J. Mol. Biol.* **272**, 790–804 (1997).
54. Matthews, C.R. Pathways of protein folding. *Annu. Rev. Biochem.* **62**, 653–683 (1993).
55. Ptitsyn, O.B. Structures of folding intermediates. *Curr. Opin. Struct. Biol.* **5**, 74–78 (1995).
56. Shortle, D., Wang, Y., Gillespie, J.R. & Wrabl, J.O. Protein folding for realists: a timeless phenomenon. *Protein Sci.* **5**, 991–1000 (1996).
57. Miranker, A.D. & Dobson, C.M. Collapse and cooperativity in protein folding. *Curr. Opin. Struct. Biol.* **6**, 31–42 (1996).
58. Aronsson, G., Mårtensson, L.-G., Carlsson, U. & Jonsson, B.-H. Folding and stability of the N-terminus of human carbonic anhydrase II. *Biochemistry* **34**, 2153–2162 (1995).
59. Teale, F.W.J. Cleavage of the haem-protein link by acid methylethylketone. *Biochim. Biophys. Acta* **35**, 543 (1959).
60. Hiraoka, Y. & Sugai, S. Equilibrium and kinetic study of sodium- and potassium-induced conformational changes of apo-α-lactalbumin. *Int. J. Pept. Protein Res.* **26**, 252–261 (1985).
61. Hughson, F.M., Wright, P.E. & Baldwin, R.L. Structural characterization of a partly folded apomyoglobin intermediate. *Science* **249**, 1544–1548 (1990).
62. Wong, K.P. & Hamlin, L.M. Acid denaturation of bovine carbonic anhydrase B. *Biochemistry* **13**, 2678–2683 (1974).
63. Jagannadham, M.V. & Balasubramanian, D. The molten globular intermediate form in the folding pathway of human carbonic anhydrase B. *FEBS Lett.* **188**, 326–330 (1985).
64. Peng, Z. & Kim, P.S. A protein dissection study of a molten globule. *Biochemistry* **33**, 2136–2141 (1994).
65. Loh, S.N., Kay, M.S. & Baldwin, R.L. Structure and stability of a second molten globule intermediate in the apomyoglobin folding pathway. *Proc. Natl. Acad. Sci. USA* **92**, 5446–5450 (1995).
66. Denisov, V.P. & Halle, B. Protein hydration dynamics in aqueous solution. A comparison of bovine pancreatic trypsin inhibitor and ubiquitin by oxygen-17 spin relaxation dispersion. *J. Mol. Biol.* **245**, 682–697 (1995).
67. Myers, J.K., Pace, C.N. & Scholtz, J.M. Denaturant *m* values and heat capacity changes: relation to changes in accessible surface areas of protein unfolding. *Protein Sci.* **4**, 2138–2148 (1995).